

# A test performance of optical fibre sensors for real-time investigations of rotational seismic events: a case study in laboratory and field conditions

Leszek R. Jaroszewicz<sup>a</sup>, Michał Dudek<sup>a\*</sup>, Anna T. Kurzych<sup>a</sup>, Krzysztof P. Teisseyre<sup>b</sup>

<sup>a</sup> Institute of Applied Physics, Military University of Technology, 2 gen. S. Kaliskiego St., Warszawa, 00-908, Poland

<sup>b</sup> Institute of Geophysics, Polish Academy of Sciences, 64 Ks. Janusza St., Warszawa, 01-452, Poland

## Article info

### Article history:

Received 20 Dec. 2021

Received in revised form 22 Dec. 2021

Accepted 24 Dec. 2021

Available on-line: 27 Dec. 2021

### Keywords:

Sagnac effect; field tests; rotational seismology; fibre optic seismograph; rotation rate; signal analysis.

## Abstract

Preliminary results of laboratory and field tests of fibre optic rotational seismographs designed for rotational seismology are presented. In order to meet new directions of the research in this field, there is clearly a great need for suitable and extremely sensitive wideband sensors. The presented rotational seismographs based on the fibre optic gyroscopes show significant advantages over other sensor technologies when used in the seismological applications. Although the presented results are prepared for systems designed to record strong events expected by the so-called “engineering seismology”, the described system modification shows that it is possible to construct a device suitable for weak events monitoring expected by basic seismological research. The presented sensors are characterized, first and foremost, by a wide measuring range. They detect signals with amplitudes ranging from several dozen nrad/s up to even few rad/s and frequencies from 0.01 Hz to 100 Hz. The performed Allan variance analysis indicates the sensors main parameters: angle random walk in the range of  $3 \cdot 10^{-8}$ – $2 \cdot 10^{-7}$  rad/s and bias instability in the range of  $2 \cdot 10^{-9}$ – $2 \cdot 10^{-8}$  rad/s depending on the device. The results concerning the registration of rotational seismic events by the systems located in Książ Castle, Poland, as well as in the coalmine “Ignacy” in Rybnik, Poland were also presented and analysed.

## 1. Introduction

Seismic methods are widely used in mining, geophysics, and civil engineering. Currently, seismic measurements are carried out mainly in the field of velocity and acceleration recording of three translational components of vibrations [1, 2]. However, knowing that the full description of the movement of a seismic wave, in addition to the aforementioned translation components, also includes three rotational components, it was necessary to take actions to measure and define the nature of the latter [3–5]. For this reason, a new strongly expanding field of science has emerged – rotational seismology. It deals with all aspects

of rotational motions induced by explosions, earthquakes, and ambient vibrations [6]. The growing belief in the value of information that may be carried by additional components of the seismic wave motion causes that rotational motions measurements are carried out not only in the case of high-energy earthquakes [7], but also, among others, in civil engineering [8–10], mining geophysics [11, 12], and even in the investigation of gravitational waves [13]. It is assumed that ground torsional movements may have a negative effect mainly on large-scale surface infrastructure facilities. Nevertheless, geophysicists studying the phenomenon of rotational waves [14, 15] have repeatedly demonstrated their effect on structures with relatively small dimensions [16–18].

Practical study of rotational seismology requires rotational seismographs with suitable parameters as is

\*Corresponding author at: [michal.dudek@wat.edu.pl](mailto:michal.dudek@wat.edu.pl)

discussed in Ref. 19. The main technical parameters are sensitivity and frequency detection band, which are different for engineering and seismological investigations. For the first one, it is about  $10^{-8}$  rad/s with detection in the range from 10 to 100 s, whereas the second one needs device operating in the frequency range of 0.01–10 Hz but with the ability to detect strong rotations as high as a few rad/s. Such a wide range of parameters can be provided by a system using the Sagnac effect [20, 21] based on a fibre optic gyroscope (FOG) with special attention to angular motion detection. Moreover, the practical testing of such device based on known disturbances is a critical issue for the future device implementation. In this paper, based on a general description of the constructed device named fibre-optic seismograph (FOS) type 5 are presented and discussed the results of its investigation in the laboratory, as well as in the field tests. The investigation was conducted for three similar devices (FOS5-01, FOS5-02, FOS5-03) designed for the engineering application and one (FOS5-04) designed for the seismological application.

## 2. FOSs construction and noise investigation in laboratory conditions

All FOS5s [see Fig. 1(a)] are constructed on the basis of a minimum optical configuration designed for FOG [Fig. 1(b)]. The main difference between FOS5-01, -02, -03 and FOS5-04 are the parameters of the sensor loop (SL). The first three use a 5-km long SL of 0.25 m diameter whereas the latter (FOS5-04) has a 14.44-km long SL with 0.61 m diameter. The SL parameters, as well as total optical losses for all FOS5 devices having the same optical power (10 mW at a wavelength of 1310 nm) are the main source for their different theoretical sensitivity. For FOS5-01, -02, -03 total transmission losses are in the range of 19.20–21.60 dB giving a theoretical sensitivity of about  $6.82 \cdot 10^{-8}$  rad/(s $\sqrt{\text{Hz}}$ ), whereas FOS5-4 with optical losses of 17.41 dB has a theoretical sensitivity of about  $1.14 \cdot 10^{-8}$  rad/(s $\sqrt{\text{Hz}}$ ), which is approx. 6-times better.

To provide extreme sensitivity, linearity, as well as operation in the required frequency range from 0.01 Hz to 100 Hz with the possibility to detect rotation rate in the range of up to a few rad/s, the FOS use the same electronic part operating in a closed-loop mode [22] based on FPGA architecture, as it is presented in Fig. 1(b). The first results of the systems investigation have been previously presented [24–26], but they are not fully satisfying. Despite the possibility of precise adjustment of the applied electronic processing to the given length of sensor loop, individual MIOC characteristics, optical power detected by APD, different frequency characteristics for FOSs are still observed.

The best results for a self-noise analysis obtained during systems investigations performed at the Military University of Technology in Warsaw, Poland, in laboratory conditions in a form of the amplitude spectral density (ASD) curves are shown in Fig. 2. All presented ASD results were filtered using a Konno-Ohmachi filter [27] with a smoothing coefficient equal to 40. The presented characteristics are the systems output of the FOSs operating at rest, when no input motion is applied and only the ambient noise is present. As it can be seen, in the required frequency range (0.01–100 Hz) FOS5-01, -02, -03 have almost flat

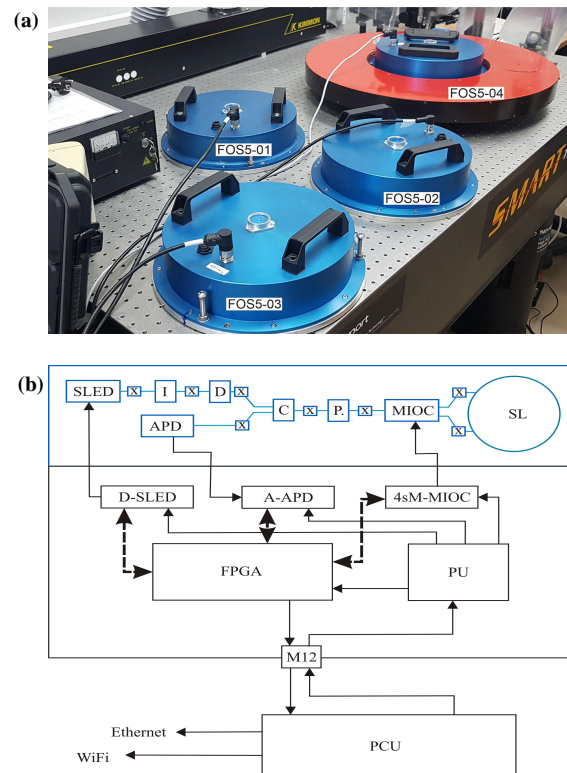


**Fig. 1.** Investigated FOSs: general FOSs view (a), general scheme of FOS construction (b): top optical part, bottom electronic part. Symbols: SLED – light source, I – fibre optic isolator, D – fibre-optic depolarizer, C – fibre-optic coupler, P – fibre-optic polarizer, MIOC – multi-integrated optical circuit, SL – sensor loop, X – fused splice, APD – avalanche photodiode, D-SLED – SLED driver, A-APD – APD amplifier, 4sM-MIOC – four-step MIOC modulator, FPGA – general FPGA unit, PU – power unit, PCU – power and communication unit [23].

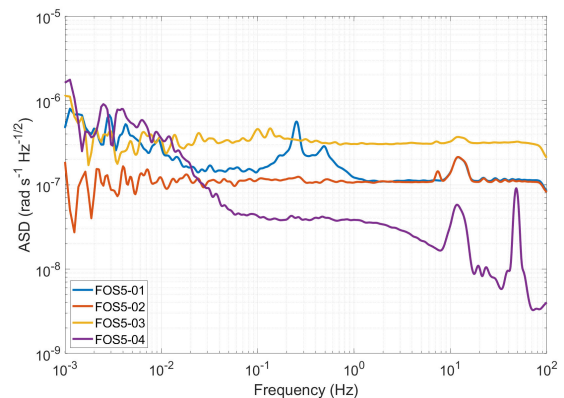


**Fig. 2.** FOSs performance across their nominal operating band as ASD noise characteristics.

characteristics, but the noise level for FOS5-03 is approx. three times higher than the other two. Because of this, the FOS5-03 has not been used in future field tests. Moreover, in the characteristics of FOS5-01, the same additional noise with the central frequency of about 0.2 Hz is evident. Also, for this device, a continuous increase of the self-noise below the frequency of 0.02 Hz can be noticed. In authors' opinion, the two aforementioned disturbances are connected with the precision of electronic parts manufacturing process, where the elements were soldered “by hand” and not in an automated manner. The noise peak with the central frequency of about 10.2 Hz, observed for all

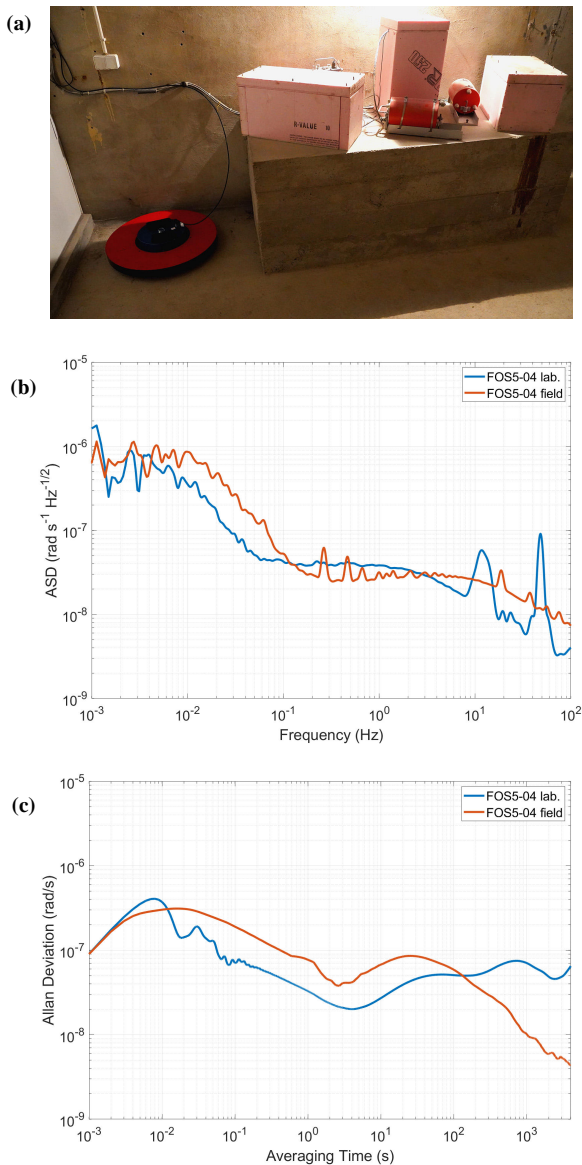


**Fig. 3.** FOS5-04 during field test in the seismological laboratory in Książ: general view of system localization (a), ASD characteristics (b), graph presenting the AV analysis (c).

FOSs, is connected with the ambient laboratory conditions, most probably coming from the actively stabilized optical table [see Fig. 1(a)].

Additionally, low-amplitude regular sharp peaks can be observed above the frequency of about 7 Hz with their amplitudes decreasing towards higher frequencies. As described by Murray-Berquist *et al.* [28], they are characteristic to all navigation-grade FOGs, and they are caused by “ramp peaks” in the raw data. These peaks can be removed by a suitable raw data processing using information of the ramp signals for a given MIOC element, although it was not possible for the presented FOS5 devices. For the FOS5-4, the observed self-noise level was of one order of magnitude lower than for other three devices, however for low frequencies, below 0.05 Hz, it increased continuously up to about  $8 \cdot 10^{-7}$  rad/(s $\sqrt{\text{Hz}}$ ) at 0.005 Hz. This increase is linked with a thermal sensitivity of this device large SL. In comparison to other FOSs, the additional high-amplitude peak with the central frequency of about 48 Hz was observed. The source of this noise was not completely identified, although it might be linked with

FOS5-04 sensitivity to acoustic sources working in the laboratory. It should be noted that the laboratory itself is located at the ground level of the main building of the Military University of Technology and, although it is far from the city centre, some of the infrastructure-based noises may be present.

### 3. Field tests regarding seismology and engineering applications

According to task 2 of the POIR 04.02.00-A003/16 project, the FOS5-04 with a theoretical sensitivity at the level of  $10^{-8}$  rad/s $\sqrt{\text{Hz}}$  was installed in the seismological observatory located in the basement of the Książ Castle near Wałbrzych, Poland [see Fig. 3(a)]. The main reason for such a localization was the exploitation of the copper ore deposit in this area, which is usually accompanied by a high level of seismic activity. Unfortunately, the recent opening of this basement to touristic activities greatly limited the possibility for seismic surveys, as only during night hours any meaningful observations are now possible. Although the new location of FOS5-04 was in a separate chamber near one of the main corridors, it was not the only device in this chamber – some other seismometers and two large containers with electronic equipment were also present. This fact greatly influenced the signals registered by FOS5-04 which may be seen in a form of the self-noise ASD analysis presented in Fig. 3(b) and, also, in the further analysis of the recorded events. Both the ASD and Allan variance (AV) analyses [29, 30] were performed on data registered in the middle of the night to remove the tourists influence.

The noise characteristics of FOS5-04 at this location is similar to the one registered in laboratory conditions, although no peaks of about 10.2 Hz and 48 Hz are visible, and additional series of disturbances in the range of 0.2–0.8 Hz are present. The ASD curve based on the field data seems to be shifted towards higher frequencies in comparison with the one for laboratory data. The AV analysis for the data collected at night shows [Fig. 3(c)] an angular random walk (ARW) equal to  $8 \cdot 10^{-7}$  rad/s and a bias instability (BI) equal to  $4 \cdot 10^{-8}$  rad/s. The first parameter represents device sensitivity (data obtained for 1 s averaging time), whereas the second one (the graph minimum in a device frequency range) represents its drift. These values for the data obtained in the Książ Castle basement are higher than for the ones registered in Warsaw, Poland where ARW was equal to  $3 \cdot 10^{-8}$  rad/s and BI was equal to  $2 \cdot 10^{-8}$  rad/s.

Nevertheless, the location of FOS5-04 makes it possible to record seismic events from surrounding area. One of such events, connected with seismic activity in a mine nearby, is shown in Fig. 4. The registered event is characterized by a strong initial amplitude of about  $0.44 \cdot 10^{-3}$  rad/s and a signal duration of about 6 s [see Fig. 4(a)]. As the FOS5 series had the low-pass filter implemented with a stopband frequency at about 170 Hz, the power spectrum and spectrogram presented in Fig. 4(b) were limited to 200 Hz even though the sampling rate of these devices was equal to 1 kHz. What is especially evident from the spectrogram [see Fig. 4(b)] and the signal [see Fig. 4(a)] analysis, some low-amplitude perturbations repeating with a period of about 0.6 s are present in the

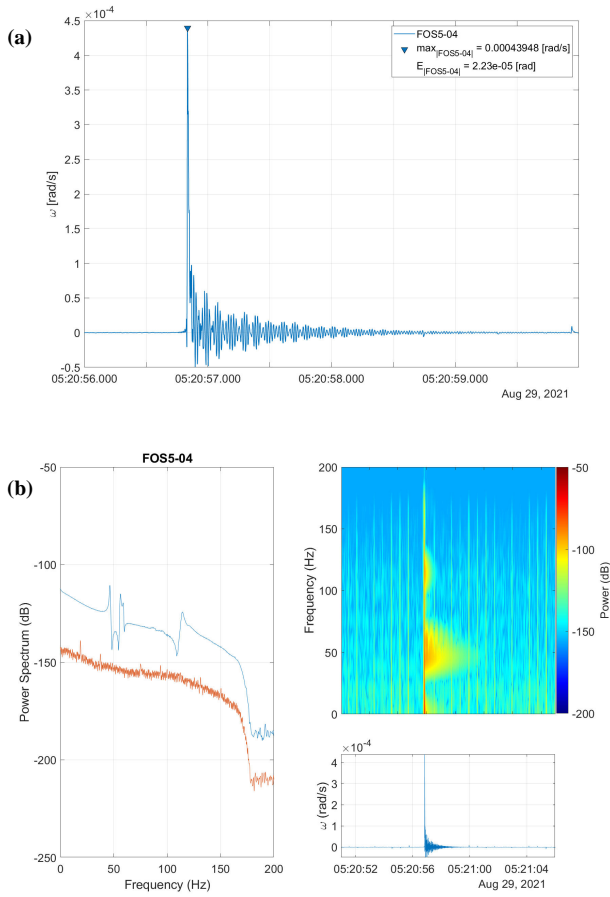


**Fig. 4.** Example of rotational events recorded at 5:20 on Aug. 29th, 2021: raw data (a), spectral characteristics (power spectra and spectrogram) of recorded signal (b).  $E$  energy coefficient calculated numerically using a method of rectangles of Riemann integral, red line at power spectra represents the noise level.

signal. As these disturbances were not visible in any of the data registered in laboratory conditions, we assume that they are intrinsic to the basement chamber, but their source was not identified yet. They may be also the reason for slightly worse ASD and AV results.

From the set of three devices designed for engineering applications, the two of them FOS5-01 and FOS5-02 have been installed on a concrete pedestal seismically isolated from the surrounding building in the historic coalmine “Ignacy” in Rybnik, Poland (see Fig. 5) in order to monitor



**Fig. 5.** General view of FOS5-01 and FOS5-02 installed at seismological platform together with another seismological device for measurements in the “Ignacy” coalmine in Rybnik.

seismic activity caused by coalmines in the Upper Silesian Coal Basin.

With regard to the spectral self-noise analysis (see data presented in Fig. 6), it can be concluded that the FOS5-02 (ARW =  $9 \cdot 10^{-8}$  rad/s, BI =  $2 \cdot 10^{-9}$  rad/s) is more precise than the FOS5-01 (ARW =  $2 \cdot 10^{-7}$  rad/s, BI =  $2 \cdot 10^{-8}$  rad/s), although both of them retained their ASD and AV characteristics similar to the ones recorded in laboratory

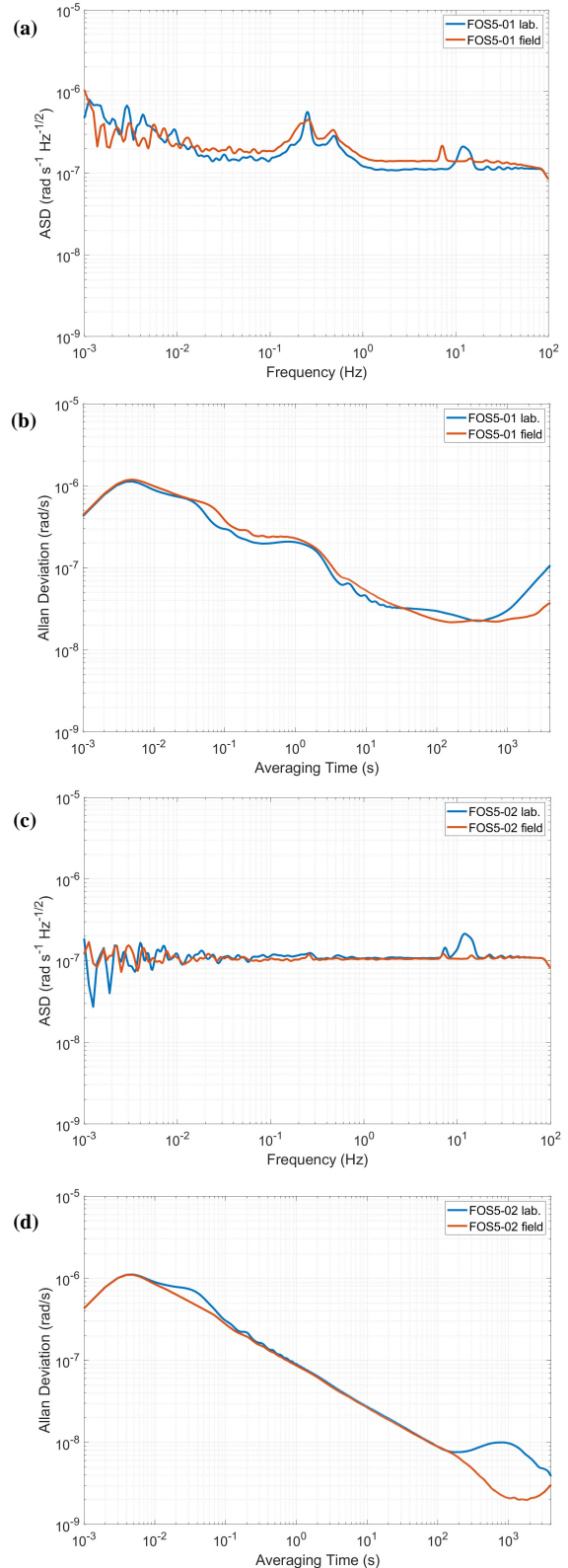


**Fig. 6.** Graphs presenting spectral analyses at Rybnik (field) and at Warsaw (lab.) localization: ASD for FOS5-01 (a), AV for FOS5-01 (b), ASD for FOS5-02 (c), AV for FOS5-02 (d).

conditions. A significant difference in the ASD curves is the lack of a peak at about 10.2 Hz for both devices. Also, low-frequency components are more stable in case of data from the field location. A slight increase in the overall ASD level of FOS5-01 may be attributed to a low long-term stability of this device, as explained further.

In case of the mining area in Rybnik, Poland, the seismic activity is not uniform. The variability of the geological structure of the area, including a lithological formation of the rocks in the vertical and horizontal profile, results in a varied number and intensity of rock bursts. For the above reason, investigations on the rotational activity in this region were the subject of task 9 of POIR 04.02.00-A003/16 project, where data collected by rotational seismographs located in the Lower Silesia were the subject of our investigations. As an example of such analysis, the rotational event recorded at 4:24 on Oct. 30<sup>th</sup>, 2021 by FOS5-01 and FOS5-02 is presented in Fig. 7.

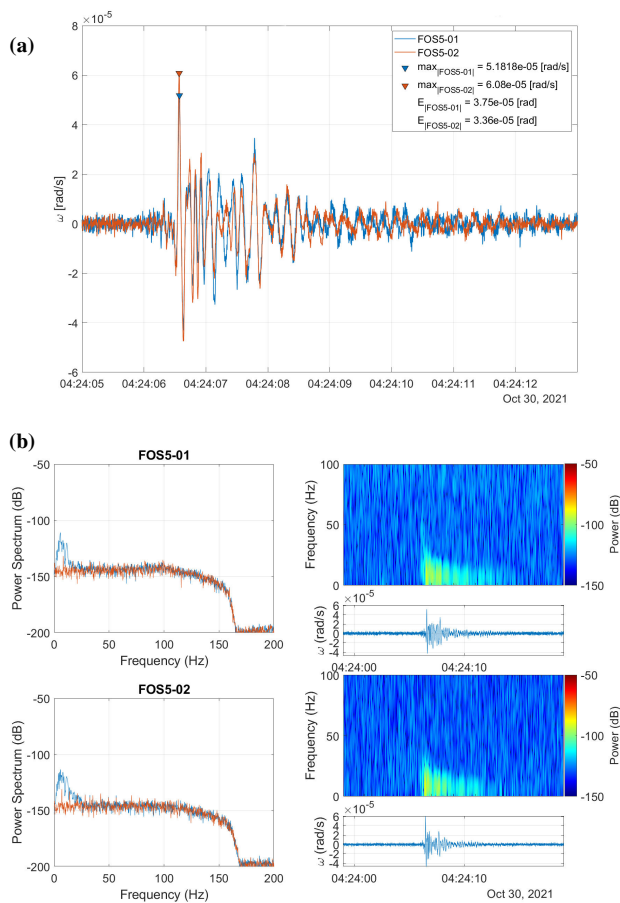


Fig. 7. Example of rotational events recorded at 4:24 on Oct. 30th, 2021: raw data with FOS5-02 moved to FOS5-1 according to correlation coefficient (a), spectral characteristics (power spectra and spectrograms) of recorded signals (b).

The maximum amplitude of the signal of the recorded event was of about 0.06 mrad/s [see Fig. 7(a)] and most of the signal spectral components were below 20 Hz [see Fig. 7(b)]. It should be noted that the presented signal from these two devices have a Pearson’s correlation coefficient equal to 0.80 which proves that the data recorded by both instruments are in good agreement.

Finally, the results related to the long-term analysis of rotation changes observed by the aforementioned devices

in their final destinations are summarized in Fig. 8. All presented data have been collected between September and October of 2021. In Fig. 8(a), the averaged rotation signals are shown, with a 50-s time window and after the subtraction of a trend line, whereas the ASD characteristics calculated for these signals are presented in Fig. 8(b). Especially for FOS5-01, we can observe a low long-term stability, caused most probably by the aforementioned production method. Due to this fact, the characteristic is smooth as for other devices and the maximum amplitude difference is about 3-times higher than for FOS5-02 and FOS5-04. An obvious feature of the data recorded by FOS5-04 is the repeating pattern of high and low averaged amplitudes, which comes from touristic activities during the day and calm nights, respectively. As it can be seen in Fig. 8(b), the presented ASD curves for all three presented in the first chart of Fig. 8(a) for FOS5-01 are different, although they have some similarities. The main difference is in the ASD level, where the best results were obtained for FOS5-02 and it is directly connected with the best stability of the device ( $BI = 2 \cdot 10^{-9}$  rad/s). The limited source of ASD differences can be also connected with different periods of the analysed data [see Fig. 8(a)]. The source of additional peaks for FOS5-01 and FOS5-02 localized at 8 o’clock, as well as for FOS5-04 at 6 o’clock will be subject to future analysis. For FOS5-04, we observed additional peaks for 60 min, 30 min, 20 min, 15 min, and 10 min, which are directly related to the touristic activity in the Książ Castle basement between 10:00 AM and 6:00 PM. However, some insights into physical phenomena can be given based on the ASD

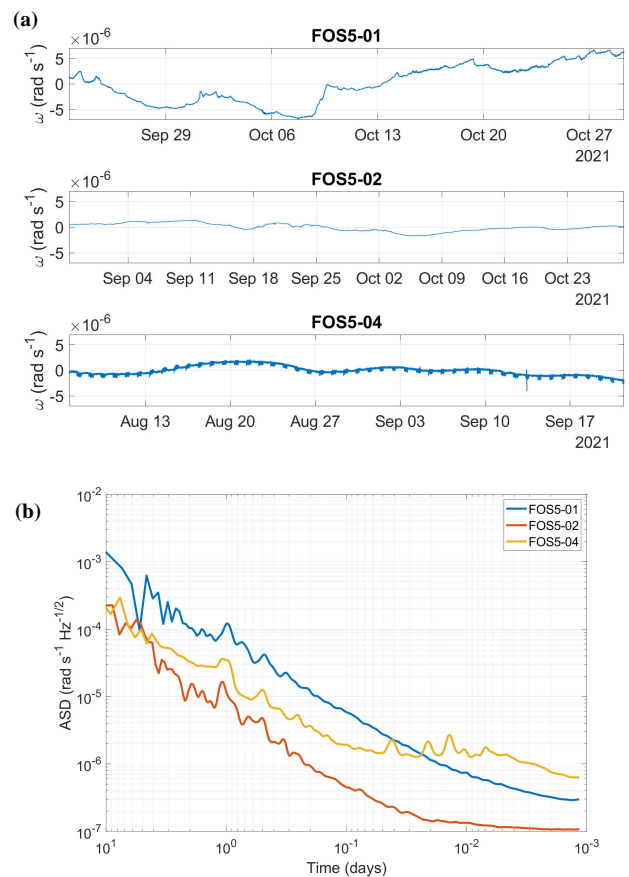


Fig. 8. Comparison of long-term signals recorded by FOS: average signal (a), ASD characteristics (b).

features repeating in all three instruments. The highest similarity is seen over a period of about a day and a half, where peaks are evident in all three ASD characteristics. Most likely, it is associated with small disturbances of the Earth's rotation rate caused by natural factors – diurnal polar motion, as well as diurnal and semidiurnal tides [31].

#### 4. Conclusions

The preliminary results in the designated locations proved that the FOS5 devices are fully capable of registering ground rotations in a whole frequency range designed for engineering seismology (strong signals with frequencies up to 100 Hz). However, because FOS5-04 uses the same electronic part and differs mainly in SL, we believe that this device is capable of detection of rotation motions with amplitude at the magnitude of  $10^{-8}$  rad/s and may be used as a universal sensor with high sensitivity in different rotational seismology applications.

In order to achieve the assumption above, an increase in attention to the electronic part preparation should be performed. Since the FOSs are made by connecting different modules, their operation is affected by different sources of interferences. The attention of module repeatability is critical which can be achieved, e.g., by automatic elements soldering.

Even though the FOS5-01 and -02 devices have some differences in analysed parameters (ASD and AV) and long-term stability, they can be used as a pair for rotation motion registration in field conditions. Despite the noise present in both systems, the signal recordings obtained from both of them are in good agreement with each other – what was shown in presented example. The correlation coefficient of analysed signal recorded by FOS5-01 and -02 is equal to 0.80, which suggests strong correlation, and can be further improved by signal post processing, e.g. by applying mean filters or low-pass filters. The main advantage of having two devices registering the same physical phenomena and located next to each other is the ability to confirm if the recorded signals are correct and not caused by malfunctioning device or selective external conditions (e.g. water droplets dripping on one of the devices). Also the probability of two FOSs malfunctioning at the same time is significantly lower than for a single system, so the recordings may be conducted continuously.

It have been also demonstrated that described instruments are capable of long-term measurements, showing results confirming positive detection of small differences in Earth's rotation rate – mainly diurnal and semi-diurnal. Authors believe that the described systems can be used not only for the seismological events monitoring, either natural or artificial, but also for long-term observations of changes in Earth's angular velocity.

#### 5. Authors' statement

Research concept and design, L.R.J and M.D.; collection and assembly of data, M.D, A.T.K. and K.P.T; data analysis and interpretation, M.D. and L.R.J; writing the article, L.R.J, A.T.K and M.D.; final approval of article, L.R.J, A.T.K, M.D and K.P.T.

#### Acknowledgements

This research was financially supported by the Ministry of the National Defence of the Republic of Poland, project GBMON/13-995/2018/WAT as well as program POIR 04.02.00-14-A003/16 “EPOS – System Obserwacji Płyty Europejskiej”.

#### References

- [1] Guéguen, P. & Astorga, A. The Torsional Response of Civil Engineering Structures during Earthquake from a Observational Point of View. *Sensors* **21**, 342 (2021). <https://doi.org/10.3390/s21020342>
- [2] Zembaty, Z., Bernauer, F., Igel, H. & Schreiber, K. U. Rotation Rate Sensors and Their Applications. *Sensors* **21**, 5344 (2021). <https://doi.org/10.3390/s21165344>
- [3] Guéguen, P., Guattari, F., Aubert, C. & LAudat. Comparing Direct Observation of Torsion with Array-Derived Rotation in Civil Engineering Structures. *Sensors* **21**, 142 (2021). <https://doi.org/10.3390/s21020142>
- [4] Rossi, Y. et al. Kalman Filter-Based Fusion of Collocated Acceleration, GNSS and Rotation Data for 6C Motion Tracking. *Sensors* **21**, 1543 (2021). <https://doi.org/10.3390/s21041543>
- [5] Fulawka, K., Pytel, W. & Pałac-Walko, B. Near-Field measurement of six degrees of freedom mining-induced terms in lower siliesian coper basin. *Sensors* **20**, 6801 (2020). <https://doi.org/10.3390/s21020142>
- [6] Lee, W. H. K. Seismology, Rotation. in *Encyclopedia of Solid Earth Geophysics*; (eds. Gupta, H. K.) 1–12 (Springer, Dordrecht, The Netherlands, 2019).
- [7] Chin-Jen, L., Chun-Chi, L. & Lee, W.H.K. Recording Rotational and Translational Ground Motions of Two TAIGER Explosions in Northeastern Taiwan on 4 March. *Bull. Seismol. Soc. Am* **99**(2B), 1237–1250 (2008). <https://doi.org/10.1785/0120080176>
- [8] Trifunac, M. D. Rotations in Structural Response. *Bull. Seismol. Soc. Am* **99**(2B), 968–979 (2009). <https://doi.org/10.1785/0120080068>
- [9] Grzebyk, W., Mertuszka, P. & Stolecki, L. Characteristics of the vibratory motion of a transaction and rotating character coming from mine seismic quakes. *Wiadomości Górnicze* **66**(2), 97–103 (2015). [in Polish]
- [10] Kurzych, A. T, Jaroszewicz, L. R., Kowalski, J. K. & Sakowicz, B. Investigation of rotational motion in a reinforced concrete frame construction by a fibre optic gyroscope. *Opto- Electron. Rev.* **28**(2), 69-73 (2020). <https://doi.org/10.24425/opehre.2020.132503>
- [11] Zembaty, Z., Mutke, G., Nawrocki, D. & Bobra, P. Rotational Ground-Motion Records from Induced Seismic Events, *Seismol. Res. Let.* **88**(1), 13-22 (2017). <https://doi.org/10.1785/0220160131>
- [12] Kaláb, Z., Knejzlík, J. & Lednická, M. Observation of rotational component in digital data of mining induced seismic events. *Górnictwo i Geologia* **7**(1), 75–85 (2012).
- [13] Ju, L., Blair, D. G. & Zhao, C. Detection of gravitational waves. *Rep. Prog. Phys.* **63**, 1317–1427 (2000). <https://doi.org/10.1088/0034-4885/63/9/201>
- [14] Teisseyre R. Why rotational seismology: confrontation between classic and asymmetric theories. *Bull. Seismol. Soc. Am.* **101**(4), 1683-1691 (2011). <https://doi.org/10.1785/0120100078>
- [15] Abreu, R., Kamm, J. & Reiß, A-S. Micropolar modelling of rotational waves in seismology. *Geophys. J. Int.* **210**, 1021-1046 (2017). <https://doi.org/10.1093/gji/ggx211>
- [16] Hart, G. C., DiJulio, R. M. & Lew, M. Torsional response of high rise buildings ASCE, *Journal of Structure Division* **101**(2), 397–415 (1975). <https://doi.org/10.1061/JSDEAG.0003999>
- [17] Suryanto, W. Rotational Motions in Seismology, Theory and Application. (LMU München: Faculty of Geosciences, 2006). [https://edoc.ub.uni-muenchen.de/7850/1/Suryanto\\_Wiwit.pdf](https://edoc.ub.uni-muenchen.de/7850/1/Suryanto_Wiwit.pdf)
- [18] Zerva, A. & Zhang, O. Corellation patterns in characteristic of spatially variable seismic ground motions. *Earthquake Engineering & Structural Dynamics* **26**, 19–39 (1997). [https://doi.org/10.1002/\(SICI\)1096-9845\(199701\)26:1%3C19::AID-EQE620%3E3.0.CO;2-F](https://doi.org/10.1002/(SICI)1096-9845(199701)26:1%3C19::AID-EQE620%3E3.0.CO;2-F)

- [19] Jaroszewicz, L.R. et al. Review of the usefulness of various rotational seismometers with laboratory results of fibre-optic ones tested for engineering applications. *Sensors* **16**, 2161, (2016). <https://doi.org/10.3390/s16122161>
- [20] Sagnac, G. The light ether demonstrated by the effect of the relative wind in ether into a uniform rotation interferometer. *Acad. Sci.* **95**, 708-710 (1913).
- [21] Post, E. J. Sagnac effect. *Rev. Mod. Phys.* **39**, 475-496 (1967). <https://doi.org/10.1103/RevModPhys.39.475>
- [22] Lefevre, H. C., Martin, P. et al. High-dynamic-range fibre gyro with all-digital signal processing. *Proc. of SPIE* **1367**, 72-80 (1991). <https://doi.org/10.1117/12.24730>
- [23] Niespodziany, S., Kurzych, A.T. & Dudek M. Detector diode circuit noise measurement and power supply method selection for the fibre optic seismograph, *Opto-Electron. Rev.* **29**(2), 71-79 (2021). <https://doi.org/10.24425/opelre.2021.135830>
- [24] Kurzych, A. T. et al. Measurements of rotational events generated by artificial explosions and external excitations using the optical fibre sensors network, *Sensors* **20**(21), 6107 (2020). <https://doi.org/10.3390/s20216107>
- [25] Bernauer, F. et al. Rotation, Strain and Translation Sensors Performance Tests with Active Seismic Sources. *Sensors* **21**, 264 (2021). <https://doi.org/10.3390/s21010264>
- [26] Kurzych, A. T., Jaroszewicz, L. R., Dudek, M., Sakowicz, B. & Kowalski, J. K. Towards uniformity of rotational events recording – initial data from common test engaging more than 40 sensors including a wide number of fibre-optic rotational seismometers. *Opto-Electron. Rev.* **29**(1), 39-44 (2021). <https://doi.org/10.24425/opelre.2021.135827>
- [27] Konno, K. & Ohmachi, T. Ground Motion characteristics estimated from spectral ratio between horizontal and vertical components of microtremor. *Bull. Seismol. Soc. Am.* **88**(1), 228-241 (1998). <https://doi.org/10.1785/BSSA0880010228>
- [28] Murray-Bergquist, L., Bernauer, F. & Igel, H. Characterization of Six-Degree-of-Freedom Sensors for Building Health Monitoring. *Sensors* **21**, 3732 (2021). <https://doi.org/10.3390/s21113732>
- [29] IEEE Standard Specification Format Guide and Test Procedure for Single-Axis Interferometric Fibre Optic Gyros. *IEEE-SA Standards Boards* 952 (1997). <https://doi.org/10.1109/IEEESTD.1998.86153>
- [30] Allan Variance: Noise Analysis for Gyroscopes. Applications Note AN5087 Rev. 0.2/2015. *Freescale Semiconductor Inc.* (2015). <https://telesems.co/wp-content/uploads/2017/05/AllanVariance5087-1.pdf>
- [31] Di Virgilio, A. D. et al. Sensitivity limit investigation of a Sagnac gyroscope through linear regression analysis. *Eur. Phys. J. C* **81**, 400 (2021). <https://doi.org/10.1140/epjc/s10052-021-09199-1>